

Structural and Physico-Chemical Elucidation of Oxovanadium(IV) and Dioxouranium(VI) Complexes of N-(Pyrrolidinobenzyl)benzamide

M. VISWANATHAN

Department of Chemistry, Sree Narayana College, Alathur, Palakkad-678 682, India
E-mail: drmvswanath@yahoo.co.in

Oxovanadium(IV) and dioxouranium(VI) complexes of N-(pyrrolidinobenzyl)benzamide (PBB) have been synthesized and characterized by elemental analyses, molar conductance, infrared spectra, magnetic susceptibility measurements, thermal, X-ray powder diffraction and antimicrobial studies. The complexes exhibit the following formulae $[\text{VO}(\text{PBB})_2] \cdot 2\text{H}_2\text{O}$ and $[\text{UO}_2(\text{PBB})_2(\text{H}_2\text{O})_2]$.

Key Words: Oxovanadium, Dioxouranium, N-(Pyrrolidinobenzyl)-benzamide, Spectral, Thermal.

INTRODUCTION

Studies of metal complexes of benzaldehyde based Mannich bases N,N'-bis(morpholinobenzyl)urea¹, piperidinobenzylurea^{2,3} and N-(morpholinobenzyl)benzamide⁴ have been reported. Another work in this field is on the complexing characteristics of the Mannich base, N-(pyrrolidinobenzyl)benzamide (PBB)⁵. In continuation of these studies the present communication reports the synthetic, structural and thermal aspects of the complexes of PBB with VO^{2+} and UO_2^{2+} ions. The kinetic parameters of thermal decomposition such as energy of activation (E), pre-exponential factor (A) and entropy of activation (ΔS) have been determined by Coats-Redfern equation. The antibacterial activities of the ligand and the complexes are also described in this communication. The structure of the ligand may be represented as in Fig. 1.

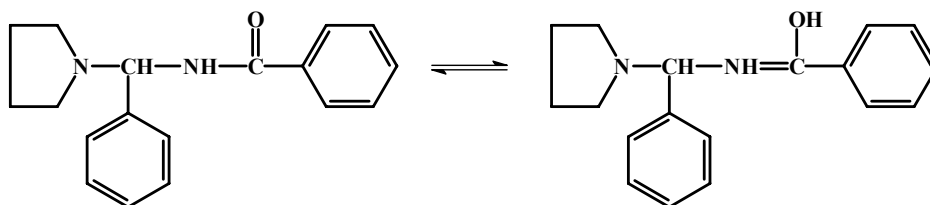


Fig. 1. N-(Pyrrolidinobenzyl)benzamide (PBB)

EXPERIMENTAL

The chemicals used were of AR grade. The solvents were double distilled before use. The ligand N-(pyrrolidinobenzyl)benzamide (PBB) was prepared by reported method⁵.

Synthesis of N-(pyrrolidinobenzyl)benzamide (PBB): Benzamide (10 mmol) in 20 mL of ethanol was mixed with pyrrolidine (10 mmol) with stirring to get a clear solution at a temperature of 10 °C. To this, benzaldehyde (10 mmol) was added in drops with stirring for *ca.* 10-20 min. The reaction mixture was kept at room temperature for 2 d. The colourless crystals were filtered and recrystallized from ethanol (yield 69.5 %; m.p. 85 °C).

Synthesis of metal complexes: A solution of PBB and the corresponding metal salt (2:1 mole ratio) in ethanol-chloroform mixture (1:6 v/v) was boiled under reflux at 58 °C (b.p of azeotropic mixture) for *ca.* 4-5 h. The resulting solution was concentrated and then cooled. The precipitated complexes were filtered, washed with ethanol and dried *in vacuo*.

The complexes were crystalline solids, stable at room temperature and non-hygroscopic. Both the complexes were soluble in DMF and DMSO. The metal contents of the complexes were determined by standard methods⁶. The molar conductance of the complexes in ethanol (*ca.* 10⁻³ M solutions) were measured at room temperature by using and ELICO conductivity bridge type CM82T with a dip type conductivity cell having platinum electrodes (cell constant = 0.94 cm⁻¹). Magnetic susceptibilities of the complexes were determined at room temperature by Guoy method. Molar masses of the complexes were determined by Rast method using biphenyl as the solvent⁷. The infrared spectra of the complexes were recorded in the range 4000-400 cm⁻¹. The TG-DTG curves of the complexes were recorded on a thermal analyzer from ambient to 850 K. The mass percentage *vs.* temperature curves obtained were redrawn in appropriate scales. Independent pyrolysis experiment in air was carried out for both the complexes and the loss of mass determined in each case was compared with that obtained from TG. Thermal decomposition kinetics of the VO(IV) complex was studied and the kinetic parameters were evaluated by Coats-Redfern method.

The X-ray powder patterns were recorded by using Philips Diffractometer (Model PW 1710) for both the complexes. The ligand and the complexes were screened for their antibacterial activity against *S. aureus*, *K. pneumonia*, *P. vulgaris* and *E. coli* by disc diffusion method⁸ at Sree Chithra Thirunal Institute for Medical Sciences and Technology, Thiruvananthapuram, India.

RESULTS AND DISCUSSION

The analytical data given in Table-1 indicate a 2:1 [M:L] stoichiometry of the complexes. The molar conductivities of the complexes (Table-2) in DMF and nitrobenzene were in the range corresponding to those of nonelectrolytes. The magnetic moment of the complex, [VO(PBB)₂]-2H₂O is found to be 1.77 BM which is close

to the spin only value of 1.73 BM corresponding to one unpaired electron⁹. The dioxouranium complex was found to be diamagnetic in nature. This may be explained on the basis of the electronic configuration of the central metal ion. The central metal ion, U⁶⁺ does not possess any unpaired electron and has the inert gas configuration.

TABLE-1
ANALYTICAL DATA OF OXOVANADIUM(IV) AND
DIOXOURANIUM(VI) COMPLEXES OF PBB

Complex	Colour	M:L ratio	Molar mass	Metal percentage
[VO(PBB) ₂].2H ₂ O	Grey	2:1	672.8 (663)	7.56 (7.69)
[UO ₂ (PBB) ₂ (H ₂ O) ₂]	Yellow	2:1	871.8 (866)	24.21 (24.97)

TABLE-2
MOLAR CONDUCTANCE DATA OF OXOVANADIUM(IV) AND
DIOXOURANIUM(VI) COMPLEXES OF PBB

Complex	Concentration × 10 ³ M	Molar conductance (ohm ⁻¹ cm ² mol ⁻¹)	
		In DMF	In Nitrobenzene
[VO(PBB) ₂].2H ₂ O	1.02	5.7	2.3
[UO ₂ (PBB) ₂ (H ₂ O) ₂]	1.01	4.9	2.5

The mass spectrum of the ligand was recorded. The base peak observed at m/z 122 shows the presence of benzamide moiety. The molecular ion peak for the ligand is observed at m/z = 280 (C₁₈H₂₀N₂O). Other important peaks at m/z = 120 and 105 correspond to the presence of C₆H₅CONH and C₆H₅CO, respectively.

The infrared spectrum of the Mannich base PBB shows ν(NH) modes at 3460 (asymmetric) and 3360 cm⁻¹ (symmetric). The carbonyl and C–N–C stretching frequencies of PBB appear at 1650 and 1160 cm⁻¹, respectively. The ν(NH) band appearing at 3460 and 3360 cm⁻¹ remain unaltered in the spectra of the complexes showing the non-participation of nitrogen of NH₂ in coordination. The band at 1160 cm⁻¹ in the ligand¹⁰, which is due to C–N–C stretching frequency, shifts to 1145-1132 cm⁻¹, in the spectra of the complexes. This shows the coordination through the tertiary nitrogen of pyrrolidine ring. The spectra of the complexes show negative shifts of the carbonyl band at 1650 to 1630-1622 cm⁻¹ indicating the coordination through the carbonyl oxygen. The infrared spectra of the dioxouranium complex shows additional bands at 3500-3470, 830-810 and 630-620 cm⁻¹ showing the presence of coordinated water¹¹. The oxovanadium complex shows an additional band around 3450 cm⁻¹ indicating the presence of water of hydration¹². The absence of absorption band around 800 cm⁻¹ shows that the water molecules are not coordinated¹¹. The asymmetric stretching frequency of O=U=O group is observed at 921 cm⁻¹ in the dioxouranium complex. A strong band at 918 cm⁻¹ in the oxovanadium complex is assigned to V=O stretching frequency of VO²⁺ unit. The additional bands in the regions 460-440 and 530-525 cm⁻¹ are assigned to ν(M–O) and ν(M–N), respectively.

The X-ray powder patterns were recorded for VO(IV) and UO₂(VI) complexes. The diffraction patterns were indexed (Table-3) by the method developed by Hesse¹³ and Lipson^{14,15}. Both the complexes are found to be orthorhombic. The cell parameters have been calculated by using the equation:

$$\sin^2 \theta(hkl) = Ah^2 + Bk^2 + Cl^2 \text{ where } A = \frac{\lambda^2}{4a^2}; B = \frac{\lambda^2}{4b^2} \text{ and } C = \frac{\lambda^2}{4c^2}.$$

TABLE-3
X-RAY DIFFRACTION DATA OF [VO(PBB)₂].2H₂O

Line	hkl	sin ² θ observed	sin ² θ calculated	Line	hkl	sin ² θ observed	sin ² θ calculated
1	10	0.0038	0.0036	19	403	0.1009	0.1014
2	1	0.0074	0.0070	20	441	0.1031	0.1030
3	120	0.0171	0.0168	21	251	0.1063	0.1066
4	21	0.0214	0.0214	22	350	0.1106	0.1116
5	121	0.0244	0.0238	23	4	0.1121	0.1120
6	301	0.0286	0.0286	24	243	0.1310	0.1302
7	320	0.0368	0.0360	25	451	0.1351	0.1354
8	31	0.0382	0.0394	26	261	0.1463	0.1462
9	131	0.0416	0.0418	27	324	0.1489	0.1480
10	222	0.0510	0.0520	28	613	0.1529	0.1530
11	330	0.0550	0.0540	29	253	0.1629	0.1626
12	40	0.0586	0.0576	30	524	0.1866	0.1864
13	331	0.0611	0.0610	31	63	0.1935	0.1926
14	430	0.0706	0.7080	32	435	0.2454	0.2456
15	213	0.0750	0.0762	33	364	0.2636	0.2632
16	422	0.0810	0.0808	34	316	0.2769	0.2772
17	223	0.0868	0.0870	35	564	0.3012	0.3016
18	432	0.0987	0.0988	–	–	–	–

The lattice constants for VO(IV) complexes are A = 0.0044, B = 0.0090 and C = 0.0798. Hence a = 17.9808 Å, b = 15.2088 Å and c = 10.6982 Å. The cell volume of the complex is given as V = abc = 2.925 × 10⁻²¹ cm³, its density is 0.8083 g cm⁻³ and the molar mass is 663. This gives n as equal to dN₀V / M = 2.147 ≈ 2. Therefore the number of molecules per unit cell is 2. For UO₂(VI) complexes the unit cell dimensions are A = 0.004934, B = 0.0115 and C = 0.0947. Hence a = 21.026 Å, b = 18.523 Å and c = 13.001. Thus, the cell volume of the complex is V = abc = 5.0634 × 10⁻²¹ cm³, density is 1.14 g cm⁻³ and the molar mass is 866. This gave n as equal to 4.013 ≈ 4. Thus, the number of molecules per unit cell is 4.

Thermal studies were conducted for both the complexes. Independent pyrolysis experiments in air were also carried out. For this a known amount of the complex was heated in a porcelain crucible upto 800 °C for ca. 1 h. From the mass of the residue, the loss of mass was calculated in each case which was compared with the percentage loss of mass obtained from the experiment.

Thermogravimetric curves of the complexes were recorded in the temperature range ambient to 800 °C (Fig. 2). For the complex $[\text{VO}(\text{PBB})_2] \cdot 2\text{H}_2\text{O}$ the TG plateau is upto 343 K indicating that the complex is stable upto 343 K. The complex decomposes in three stages. The first stage of decomposition is from 343 to 473 K. The peak temperature at this stage is 362 K. The mass loss at this stage is about 5.5 % which corresponds to the loss of water molecules from the complex. The loss of water molecules at this low temperature shows that they are lattice held^{16,17}. The second stage of decomposition is from 519 to 591 K. The summit temperature as given by DTG curve is 568 K. During this stage a weight loss of 62.85 % occurs. This weight loss is due to the release of $\text{C}_6\text{H}_5\text{CO}-\text{NCH}-\text{C}_6\text{H}_5$ parts of the organic moiety which corresponds to a theoretical loss of mass equal to 63.05 %. The third stage of decomposition extends from 691 to 748 K. The peak is obtained at 742 K. The weight loss during this interval is only 21.24 %. This is due to the release of the remaining portion of the organic moiety which would theoretically produce a mass loss of 21.4 %. The TG curve shows the second plateau after 748 K indicating the completion of decomposition. The last two stages of decomposition are attributed to the complete removal of the ligand from the complex. The residual mass of 13.81 % is due to the stable metal oxide which is in conformity with the data of independent pyrolysis (13.94 %) and the theoretical value (13.72 %).

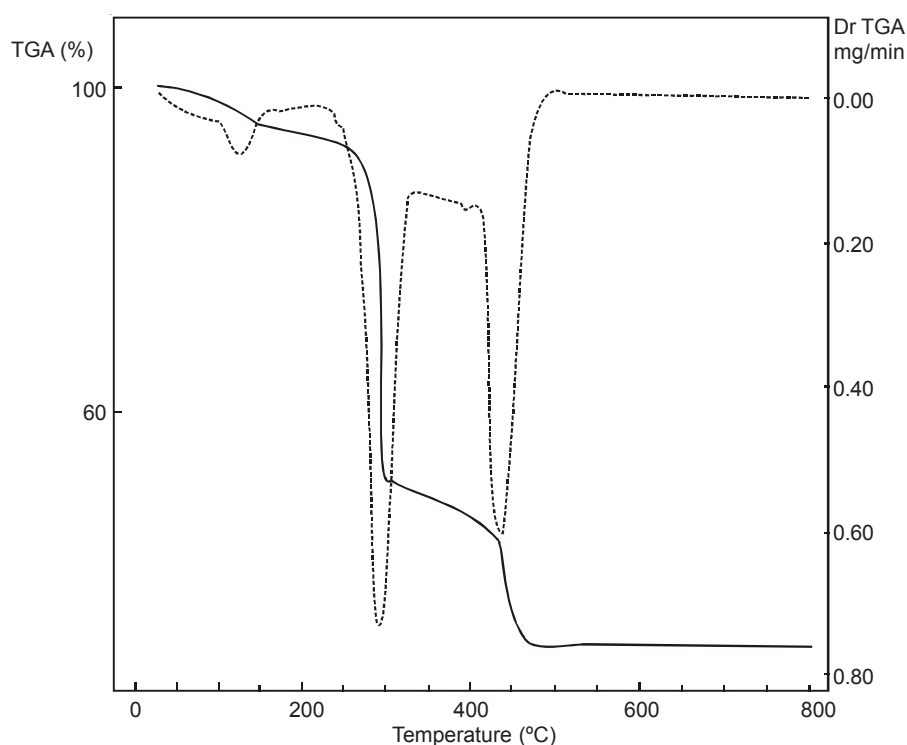


Fig. 2. TG and DTG curves for the thermal decomposition of $[\text{VO}(\text{PBB})_2] \cdot 2\text{H}_2\text{O}$

For the complex [UO₂(PBB)₂(H₂O)₂], the TG curve shows three stages of decomposition. The first stage of decomposition takes place in the range of 430-460 K with a mass loss of 4.48 % (calculated 4.2 %) which corresponds to two molecules of coordinated water¹⁸. The summit temperature as given by the DTG curve is 449 K. The second stage of decomposition is from 490 to 610 K. The summit temperature at this stage is 579 K. At this stage, a mass loss of 47.6 % occurs which corresponds to the release of C₆H₅-CO-NCH-C₆H₅ parts of the ligand which would theoretically produce a mass loss of 48.27 %. The third stage of decomposition is from 640 to 730 K. The DTG curve gives the peak at 698 K. The mass loss at this stage is 15.9 % which is due to the release of the remaining portion of the ligand which corresponds to a theoretical loss of mass equal to 16.4 %. The TG curve shows a second plateau at 730 K which indicates the completion of decomposition. The residual mass of 32.68 % (theoretical 32.4 %) shows that the final decomposition product is the stable oxide, U₃O₈. The phenomenological data for the decomposition the complexes are given in Table-4.

TABLE-4
PHENOMENOLOGICAL DATA OF DECOMPOSITION OF THE COMPLEXES

Complex	Stage of decomposition	T _i (K)	T _f (K)	T _s (K)	Mass loss (%)
[VO(PBB) ₂].2H ₂ O	I	343	473	362	5.50
	II	519	591	568	62.85
	III	601	691	659	21.24
[UO ₂ (PBB) ₂ (H ₂ O) ₂]	I	430	460	449	4.48
	II	490	610	579	47.60
	III	640	730	698	15.90

The Coats-Redfern plots of $\log\left(\frac{g(\alpha)}{T^2}\right)$ vs. $1/T$ of oxovanadium(IV) complex data at different stages of decomposition was used to evaluate the kinetic parameters (Tables 5-8). The kinetic parameters were evaluated by the Coats-Redfern equation:

$$\log \frac{g(\alpha)}{T^2} = \log \left(\frac{AR}{\phi E} (1 - 2RT/E) \right) - \frac{E}{2.303RT}$$

Since $\frac{2RT}{E} \ll 1$, it may be neglected. So the plot of $\log g(\alpha)/T^2$ vs. $1/T$ should give a straight line with slope $-\frac{E}{2.303R}$. From this, E , *i.e.*, the energy of activation can be calculated. The pre-exponential factor, A , is calculated from the intercept, $\log \frac{AR}{\phi E}$. The entropy of activation, ΔS was calculated with the help of the relation,

TABLE-5
DATA USED TO EVALUATE KINETIC PARAMETERS FOR
DECOMPOSITION OF $[\text{VO}(\text{PBB})_2] \cdot 2\text{H}_2\text{O}$: STAGE 1

α	$g(\alpha)$	T (K)	$1/T \times 10^3$	$\log [g(\alpha)/T^2]$
0.2216	0.2504	363	2.7548	-5.72140
0.3235	0.3909	383	2.6110	-5.77440
0.4875	0.6685	403	2.4813	-5.38520
0.6522	1.0560	423	2.3641	-5.52292
0.8237	1.7352	443	2.2573	-5.05360
0.9116	2.4272	463	2.1598	-4.94620

TABLE-6
DATA USED TO EVALUATE KINETIC PARAMETERS FOR
DECOMPOSITION OF $[\text{VO}(\text{PBB})_2] \cdot 2\text{H}_2\text{O}$: STAGE 2

α	$g(\alpha)$	T (K)	$1/T \times 10^3$	$\log [g(\alpha)/T^2]$
0.0391	0.0399	529	1.8903	-6.8478
0.1038	0.1095	539	1.8553	-6.4230
0.2079	0.2331	549	1.8215	-6.1119
0.3376	0.4118	559	1.7889	-5.8801
0.6105	0.9428	569	1.7575	-5.5357
0.8570	1.9457	579	1.7271	-5.2364

TABLE-7
DATA USED TO EVALUATE KINETIC PARAMETERS FOR
DECOMPOSITION OF $[\text{VO}(\text{PBB})_2] \cdot 2\text{H}_2\text{O}$: STAGE 3

α	$g(\alpha)$	T (K)	$1/T \times 10^3$	$\log [g(\alpha)/T^2]$
0.2728	0.3186	701	1.4265	-6.1884
0.5637	0.8292	711	1.4065	-5.7851
0.7476	1.3766	721	1.3870	-5.5772
0.9092	2.3978	731	1.3680	-5.3382
0.9637	3.3142	741	1.3495	-5.2193

TABLE-8
KINETIC PARAMETERS FOR THE THERMAL
DECOMPOSITION OF $[\text{VO}(\text{PBB})_2] \cdot 2\text{H}_2\text{O}$

Stage of decomposition	E (kJ mol ⁻¹)	A (s ⁻¹)	ΔS (JK ⁻¹ mol ⁻¹)
1	25.857	8.428×10^2	-287.2172
2	191.348	2.461×10^{17}	-13.0776
3	236.987	1.045×10^{17}	-22.0561

$A = \frac{kTs}{h} e^{\Delta S/R}$, where k = Boltzmann constant, h = Planck's constant, ΔS = entropy of activation, Ts = DTG peak temperature or summit temperature and R is the gas constant. This may be rearranged to,

$$\log A = \log \frac{kTs}{h} + \frac{\Delta S}{R}$$

The α values were obtained from the TG curves. The values of kinetic parameters obtained from the linear graphs for $g(\alpha)/T^2$ vs. $1/T$ for the various stages of decomposition of the oxovanadium complex are given in Table-8.

The results of the antibacterial studies are summarized in Table-9. The metal chelates exhibit higher activity than the free ligand towards the organisms studied viz., *S. aureus*, *K. pneumonia*, *P. vulgaris* and *E. coli*. The increase in antimicrobial activity is due to faster diffusion of metal complexes through the cell membrane or due to the combined activity of the metal and the ligand. The increased activity of the metal chelates may be explained by the overtone concept¹⁹ and the Tweedy's chelation theory²⁰. The lipid membrane that surrounds the cell favours the passage of only lipid soluble materials. Thus, lipophilicity is an important factor that controls the antimicrobial activity. Due to the overlapping of the ligand orbital and partial sharing of the positive charge of the metal ion will be reduced by chelation. Chelation will also increase the delocalization of the π -electron over the whole chelate ring which enhances the lipophilicity of the complexes. As a result of this increase in lipophilicity, the penetration of the complexes into the lipid membrane is get enhanced. This in turn blocks the metal binding sites in the enzymes of micro-organisms. The results also indicate that the ligand and both the oxovanadium(IV) and dioxouranium(VI) complexes showed enhanced antibacterial activity towards *S. aureus* and *K. pneumonia*.

TABLE-9
ANTIBACTERIAL ACTIVITY AGAINST THE LIGAND AND
THE METAL COMPLEXES

Compound	Diameter of zone of inhibition (mm)							
	<i>S. aureus</i>		<i>K. pneumonia</i>		<i>P. vulgaris</i>		<i>E. coli</i>	
Quantifying	10	15	10	15	10	15	10	15
PBB	22	24	18	20	8	12	10	12
VO(IV)	26	28	22	30	12	14	12	16
UO ₂ (VI)	24	29	22	28	14	16	14	18

On the basis of the above studies, it may be concluded that the formula of the oxovanadium(IV) complex with PBB is [VO(PBB)₂].2H₂O. Thus, the coordination number of vanadium in this complex is 5. The experimental evidences confirm that the formula of the dioxouranium(VI) complex with PBB is, [UO₂(PBB)₂(H₂O)₂]. So, the coordination number of uranium in the complex is 8. The spectral and thermal studies show the presence of coordinated water in dioxouranium(VI) complex and the lattice water in oxovanadium(IV) complex.

ACKNOWLEDGEMENTS

The author is thankful to the Head, RSIC, IIT Madras, Chennai for thermal, spectral and magnetic measurements; The Director, RRL, Thiruvananthapuram for X-ray powder pattern and The Director, Sree Chithra Thirunal Institute of Medical Sciences, Poojappura, Thiruvananthapuram for antibacterial studies.

REFERENCES

1. G.V. Prabhu, Ph.D. Thesis, Bharathidasan University, (1991).
2. G.V. Prabhu and D. Venkappayya, *J. Indian. Chem. Soc.*, **72**, 511 (1995).
3. M. Viswanathan and G. Krishnan, *Asian J. Chem.*, **16**, 156 (2004).
4. N. Raman, R. Vimalaramani and C. Thangaraja, *Indian J. Chem.*, **43A**, 2357 (2004).
5. M. Viswanathan, *Asian J. Chem.*, **16**, 1039 (2004).
6. A.I. Vogel, *A Text Book of Quantitative Inorganic Analysis*, John Wiley & Sons, New York (1963).
7. W.G. Palmer, *Experimental Physical Chemistry*, The University Press, Cambridge (1954).
8. M.J. Pekzar, E.C.S. Chan and N.R. Krieg, *Microbiology*, New York, edn. 5 (1998).
9. R.L. Dutta and A. Syamal, *Elements of Magnetochemistry*, Affiliated East-West Press, New Delhi, India (1992).
10. I.J. Bellamy, *The Infrared Spectra of Complex Molecules*, Methuen, London, edn. 2 (1958); R.M. Silverstein, G.C. Bassler and T.C. Morrill, *Spectrophotometric Identification of Organic Compounds*, Wiley, New York, edn. 4 (1981).
11. K. Nakamoto, *Infrared and Raman Spectra of Inorganic and Coordination Compounds*, Wiley Interscience, New York, edn. 3 (1978).
12. C.M. Mikulski, L. Mattuci, Y. Smith, T.B. Tran and N.M. Karayannis, *Inorg. Chem. Acta*, **80**, 127 (1983).
13. R. Hesse, *Acta Crystallogr.*, **1**, 200 (1948).
14. H. Lipson, *Acta Crystallogr.*, **2**, 43 (1949).
15. H. Lipson and H. Steeple, *Interpretation of X-ray Powder Patterns*, MacMillan, London (1979).
16. J.R. Allan and P.M. Veitch, *Thermal Anal.*, **27**, 3 (1983).
17. A.N. Nikolaev, V.A. Logvinenko and L.I. Mychina, *Thermal Analysis*, Academic Press, New York, Vol. 2 (1969).
18. B. Singh, B.B. Agarwala, P.L. Mourya and A.K. Dey, *J. Indian Chem. Soc.*, **59**, 1130 (1982).
19. N. Dharmaraj, P. Viswanathamurthi and K. Natarajan, *Transition Met. Chem.*, **26**, 105 (2001).
20. L. Mishra and V.K. Singh, *Indian J. Chem.*, **32A**, (1997).

(Received: 7 March 2008;

Accepted: 4 March 2009)

AJC-7316